Geochemical Perspectives Letters



# Origin of radiogenic $^{129}$Xe variations in carbonaceous chondrites

**G. Avice, M.M.M. Meier, Y. Marrocchi**

## Supplementary Information

The Supplementary Information includes:

- Analytical Methods
- Cosmogenic and Radiogenic Contributions
- Tables S-1 and S-2
- Figures S-1 to S-5
- Supplementary Information References

## Analytical Methods

Noble gases were released from bulk fragments of Tarda, Orgueil and Tagish Lake meteorites in two extraction steps using a heating laser diode (λ=1064 nm). The first extraction step used medium laser power (1 A). The final steps were done at high laser power (5 A) until complete melting of the sample was observed. Each extraction step lasted 2 min. After extraction, reactive gases were purified sequentially using three getters (one containing V-Cr-Fe pellets and two containing Ti sponge) operated at high temperature during 5 min (300 and 800 °C for the pellets and the Ti-sponge, respectively) and cooled down to room temperature during 10 min. After removal of reactive gases, noble gases were adsorbed during 15 min on a charcoal cooled down to 10 K by a cryopump. Noble gases were then sequentially released from the charcoal by heating the cryotrap with a resistance wire. Noble gases were exposed to a D100 Capacitorr® SAES getter for 15 min before being admitted in the Noblesse® noble gas mass spectrometer. Neon isotopes were detected in multi-collection mode using three electron multipliers. $^{40}Ar^{+}$, $CO_2^{+}$ signals were also measured between each neon integration cycles to correct for $^{40}Ar^{++}$ (m = 20) and $CO_2^{++}$ (m = 22) interferences on neon signals. These corrections were applied by using the double ionisation ratios ($^{40}Ar^{++}/^{40}Ar^{+}$=10.5 % and $CO_2^{++}/CO_2^{+}$=1.2 %). Argon isotopes were measured in multi-collection mode using a faraday cup for $^{40}$Ar and electron multipliers for $^{38}$Ar and $^{36}$Ar. Krypton and xenon isotopes were measured in peak-jumping mode using an electron multiplier.

The sensitivity and the reproducibility of the instrument were determined by measuring known amounts of noble gases in aliquots taken from a standard bottle prepared from ambient air. Analytical blanks were measured repeatedly over the course the analytical session and were negligible: $2.9\times10^{-14}$ cm$^3$ STP of $^{22}$Ne *i.e.* <0.2 % of the $^{22}$Ne released during one extraction step, $1.01\times10^{-11}$ cm$^3$ STP of $^{36}$Ar *i.e.* <2 % $^{36}$Ar released during one extraction step, $7.49\times10^{-14}$ cm$^3$ STP of $^{84}$Kr *i.e.* <1 % of the $^{84}$Kr released during one extraction step and $3.65\times10^{-15}$ cm$^3$ STP of $^{130}$Xe *i.e.* <1 % of

the $^{130}$Xe released during one extraction step). All data have been corrected for blank contributions and mass discrimination of the instrument. Errors on isotope ratios include internal errors, external errors assessed by repeated measurements of standard aliquots and errors on the blank contribution.

## Cosmogenic and Radiogenic Contributions

### Presence and isolation of cosmogenic Ne

In all three meteorites analysed here, the cosmogenic component is resolvable only in Ne (it might be resolvable in He, too, which was not measured). All 12 samples show a slight excess of $^{21}$Ne relative to the dominant trapped Ne component. The latter is likely a mixture between the planetary component phase Q (*e.g.*, Busemann *et al.*, 2000) and presolar components including P3, Ne-HL and Ne-E (*e.g.*, Ott, 2014). The observed $^{21}$Ne-excesses are due to cosmogenic Ne (*i.e.* Ne produced by cosmic-ray-induced spallation of Mg, Si, Al), the concentration of which can be determined using a two- or three-component-deconvolution approach, provided the isotopic compositions of the end-members are known. Interestingly, three of the Tarda samples and both Tagish Lake samples (samples = total gas released in the 1A and 5A extractions) plot very close to a single line in the Ne-three-isotope diagram (Fig. 1), which can be extrapolated to $^{20}$Ne/$^{22}$Ne ~ 7.5 at $^{21}$Ne/$^{22}$Ne ~0.03. That value likely represents the isotopic composition of the characteristic mixture of presolar and planetary components in both Tarda and Tagish Lake. It is remarkable that the samples from both meteorites plot on the same line, with no discernible difference – this could suggest that both Tarda and Tagish Lake sample the same source material. A fourth Tarda sample plots slightly below that trend line, perhaps suggesting sample heterogeneity. On the other hand, the two Orgueil samples plot significantly above that line, indicating the additional presence of a $^{20}$Ne-rich component, which could be, e.g., implanted solar wind or a higher relative contribution of Ne-Q. Extrapolating the Tarda / Tagish Lake trend-line towards the cosmogenic end-member might potentially reveal its $^{22}$Ne/$^{21}$Ne ratio (while the $^{20}$Ne/$^{22}$Ne-ratio of cosmogenic Ne can be assumed to be constant at ~0.81 according to the model calculations of Leya and Masarik, 2009). The cosmogenic $^{22}$Ne/$^{21}$Ne-ratio is often used to determine the production rate of cosmogenic $^{21}$Ne (the "$^{22}$Ne/$^{21}$Ne-$^{21}$Ne-method" of cosmic-ray exposure (CRE) age dating, *e.g.*, Leya and Masarik, 2009). For the same chemical composition, higher values of that ratio are associated with lower shielding in smaller meteoroids, while lower values are associated with higher shielding in larger meteoroids. The shielding (essentially, the amount of material between a target meteorite sample and the cosmic-ray source) determines the production rate of $^{21}$Ne, which increases from the meteoroid surface towards the interior, reaches its maximum a few 10 cm below the surface, and eventually tails off towards zero deep inside a large meteoroid (see Fig. S-3). However, extrapolation of the Tarda/Tagish Lake trend-line to $^{20}$Ne/$^{22}$Ne = 0.81 yields a cosmogenic $^{22}$Ne/$^{21}$Ne of ~1.0, which is nominally below the expected range of 1.09-1.22 (Fig. S-3), but the associated uncertainties are likely to be large. Therefore, as is characteristic for primitive carbonaceous chondrites (*e.g.*, Krietsch *et al.*, 2021), the trapped Ne component is so dominant in all three meteorites that the $^{22}$Ne/$^{21}$Ne-ratio of the cosmogenic end-member cannot be reliably determined. Therefore, we will only be able to give a very rough estimate of the shielding (based on estimated meteoroid sizes), the $^{21}$Ne production rates and thus the CRE ages of the three meteorites.

## Meteoroid sizes and cosmogenic $^{21}$Ne production rates

As shown in Figure S-3, the expected $^{22}$Ne/$^{21}$Ne ratios and $^{21}$Ne production rates (based on the carbonaceous chondrite model from Leya and Masarik, 2009, with target chemistry changed to reflect the composition of Tarda / Tagish Lake, see Marrocchi *et al*,. 2021) show some clear variability as a function of shielding position (the surface is located at the top left end of the lines shown in Fig. S-3), but also as a function of overall meteoroid size (note that all given radii have been recalculated for a density of 1.5 g cm$^{-3}$ typical for Tarda / Tagish Lake, Brown *et al.*, 2000). Meteoroid size has only been reliably determined for Tagish Lake, where it was given as 2-3 m in radius (Brown *et al.*, 2000; blue lines in Fig. S-3). Only about 10 kg of material were found on the surface within a 16 km × 3 km strewn field (corresponding to 0.005 % - 0.02 % of the initial mass). For Orgueil, which was reported as a very bright fireball (visible over several 100 km, similar to Tagish Lake), about 14 kg were delivered to the surface within a 20 km × 4 km strewn field (Gounelle and Zolensky, 2014). Given very similar physical properties (density, porosity, low coherence, *etc*.), we can probably assume that this indicates that the Orgueil meteoroid was at least as large as the Tagish Lake meteoroid. For Tarda, only about 4 kg were found on the surface, the strewn field is only about 3 km long, and the fireball was not exceptionally bright. This suggests, to first order, that the Tarda meteoroid was smaller than the Orgueil or Tagish Lake ones, although given the similar masses found, it seems very unlikely that it would be several orders of magnitude smaller (typical ablation rates of 27-99.9 % with a median of 85 %, determined for mostly small ordinary chondrites with initial masses of 10-1000 kg (Bhandari *et al.*, 1980), are not directly applicable to these friable and - certainly in the case of Tagish Lake and Orgueil - metre-sized, multi-ton meteoroids). Still, we cannot technically exclude the smallest meteoroid sizes at this point, and determine a $^{21}$Ne production rate range of (0.11-0.28) x 10$^{-8}$ cm$^3$ STP g$^{-1}$ Ma$^{-1}$ for Tarda. For Tagish Lake, the known radius of the Tagish Lake meteoroid allows for a slightly more constrained $^{21}$Ne production rate range, of (0.13-0.23) × 10$^{-8}$ cm$^3$ STP g$^{-1}$ Ma$^{-1}$. For Orgueil, we use the basic carbonaceous chondrite model by Leya and Masarik (2009), which was calculated for CI-chondrite chemistry (not shown in Fig. S-3) and adopt a slightly lower $^{21}$Ne production rate range of (0.11-0.20) × 10$^{-8}$ cm$^3$ STP g$^{-1}$ Ma$^{-1}$.

## Cosmic-ray exposure ages

Cosmic-ray exposure ages (or age ranges) are calculated by dividing the cosmogenic $^{21}$Ne concentration by the production rate, or in this case, by the production rate range. The cosmogenic concentrations are consistent (within uncertainties) between the two samples of Orgueil, and the two samples of Tagish Lake. Within Tarda, we found two different sets of concentrations among the four samples, with the lower concentration set (Tarda B and D) having about 50 % of the cosmogenic $^{21}$Ne compared to the higher concentration set (Tarda A and C). Since the concentration of trapped gases is also lower in the lower concentration set, it is possible that both Tarda B and D lost some of their Ne, in a similar fashion. The most straightforward explanation is that these samples contained fusion crust (and were thus partially degassed), the presence of which is difficult to recognise under the microscope due to the dull-black coloration of the interior of Tarda fragments. However, differences due to a different target chemistry (*e.g.*, carbonates or anorthite) cannot be fully excluded. At this point, we exclude the two samples from the CRE age determination (see Table S-2). The CRE ages are given in Table S-2 – note that since we use the full range of possible production rates, the true CRE ages must be somewhere in-between the T21$_{low}$ and T21$_{high}$ ages given.

## Radiogenic Ar

The $^{40}$Ar/$^{36}$Ar ratios in all measured samples are clearly non-terrestrial at ~9-14. Although the measured $^{38}$Ar/$^{36}$Ar ratios are compatible with both extra-terrestrial trapped or atmospheric ratios, and thus a small contribution from (adsorbed)

atmospheric Ar cannot be conclusively excluded, we can at least determine upper limits to the K-Ar radiogenic gas retention (RGR) ages of the samples by assuming all of their $^{40}$Ar is radiogenic. We adopt K concentrations of 660, 650 and 550 ppm for Tarda, Tagish Lake and Orgueil, respectively (Brown *et al.*, 2000; Marrocchi *et al.*, 2021). This results in the K-Ar (upper limit) ages given in the R40 column in Table S-2. The values are given without uncertainty since the inter-sample variation provides a better estimate of the reproducibility of the RGR age than the precision to which the $^{40}$Ar was measured.

# Supplementary Tables

**Table S-1** Elemental abundances (in units of $cm^3$ STP $g^{-1}$) and isotopic compositions of Ne, Ar, Kr & Xe extracted from Tarda, Tagish Lake and Orgueil samples analysed in this study. Heating steps 1 & 2 correspond to laser power of 1 and 5 A, respectively. Uncertainties correspond to 1σ.

Table S-1 is available to download (Excel) from the online version of the article at https://doi.org/10.7185/geochemlet.2228

**Table S-2** Cosmogenic concentrations, production rates, exposure ages. $^{21}Ne_{cos}$: Concentration of cosmic-ray produced $^{21}Ne$, in units of $10^{-8}$ $cm^3$ STP $g^{-1}$. P21: Estimated likely range of the production rate of $^{21}Ne$, in units of $10^{-8}$ $cm^3$ STP $g^{-1}$ $Ma^{-1}$. T21: Cosmic-ray exposure age, low- and high-end estimate, in Ma. R40: Upper limit on the K-Ar RGR age, in Ga. *Two samples from Tarda did not release as much Ne as the others, probably because they contained fusion crust (see main text). 1σ uncertainties.

| Sample | $^{21}Ne_{cos}$ | P21 | $T21_{low}$ | $T21_{high}$ | R40 |
|---|---|---|---|---|---|
| Tarda A | 1.40±0.34 | 0.13-0.28 | 5.0±1.2 | 12.7±3.0 | 2.59 |
| Tarda B | 0.60±0.15* | 0.13-0.28 | - | - | 2.68 |
| Tarda C | 1.24±0.31 | 0.13-0.28 | 4.4±1.1 | 11.3±2.8 | 2.61 |
| Tarda D | 0.55±0.14* | 0.13-0.28 | - | - | 2.44 |
| Tagish Lake A | 1.16±0.29 | 0.13-0.23 | 5.0±1.3 | 8.9±2.2 | 2.84 |
| Tagish Lake B | 0.99±0.25 | 0.13-0.23 | 4.3±1.1 | 7.6±1.9 | 2.05 |
| Orgueil A | 1.22±0.32 | 0.11-0.20 | 6.1±1.6 | 11.1±2.9 | 2.69 |
| Orgueil B | 1.21±0.32 | 0.11-0.20 | 6.1±1.6 | 11.0±2.9 | 2.22 |

## Supplementary Figures

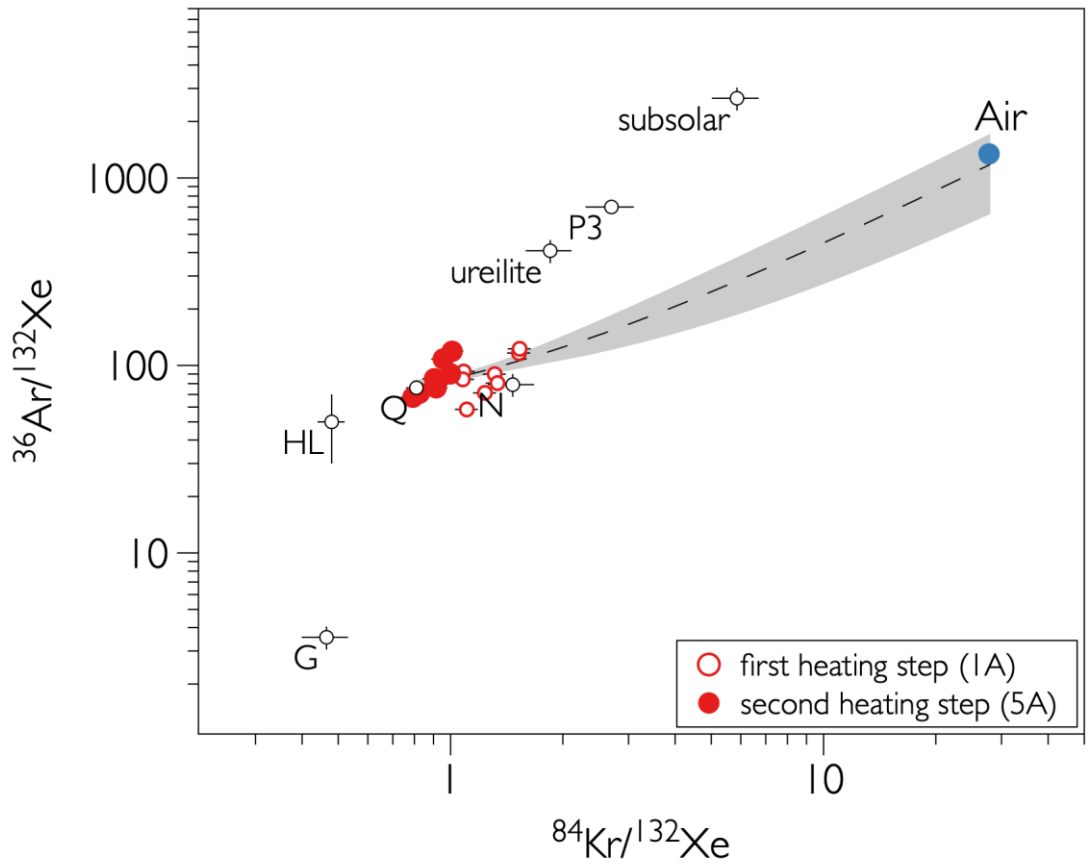


**Figure S-1** Elemental abundance ratios for samples measured in this study. For clarity, samples are not identified and only first and second heating steps are represented. Low temperature heating steps plot toward the Air component. The dashed line and grey area (±1σ) correspond to a linear fit through the entire dataset. High temperature heating steps plot close to the Q component. Figure adapted from Ott (2002). See also Ott (2002) for references for the elemental ratios of primordial components in the Solar System.

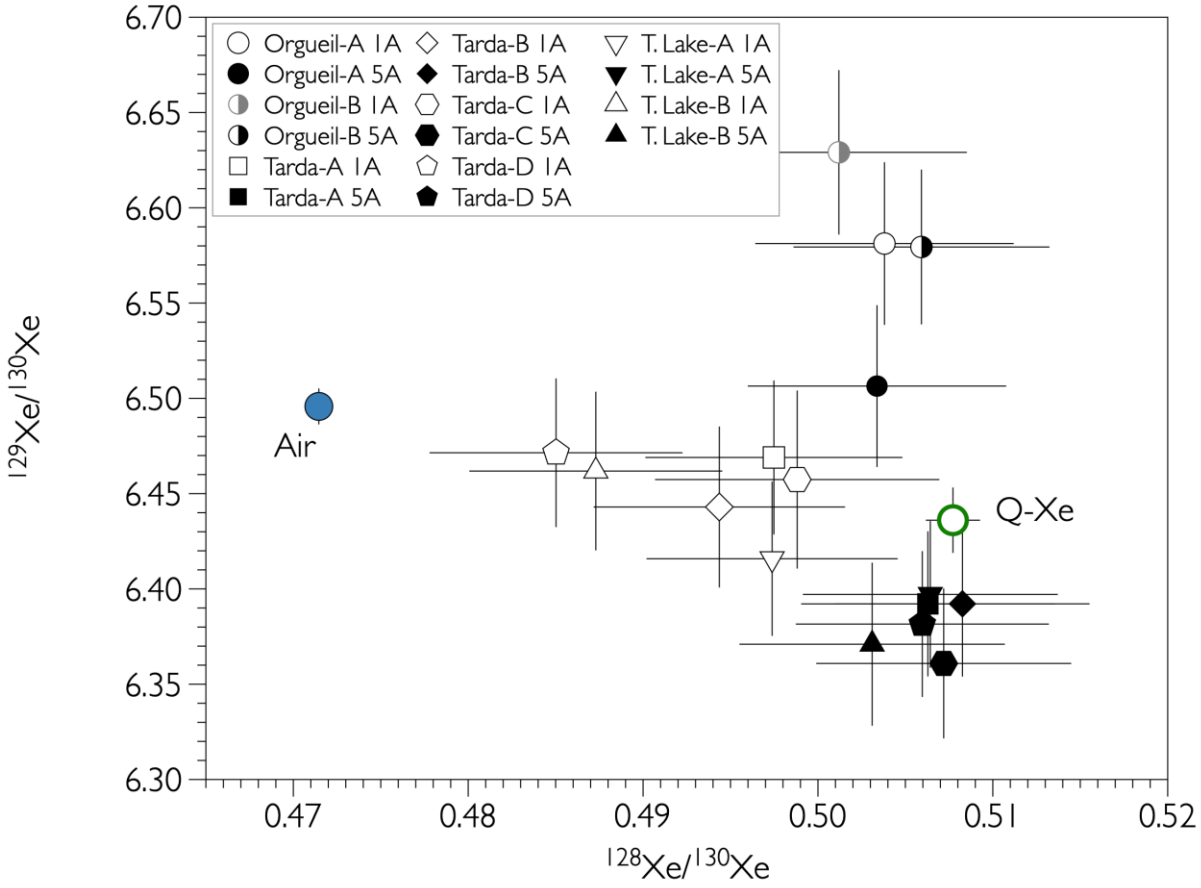


**Figure S-2** Three-isotope plot of xenon. Low temperature heating steps show a tendency toward atmospheric xenon (Air, Ozima and Podosek, 2002). Xenon released during high temperature heating steps of Tarda and Tagish Lake samples has a $^{129}Xe/^{130}Xe$ ratio systematically lower than the Q component (Busemann *et al.*, 2000). Errors are at 1σ.

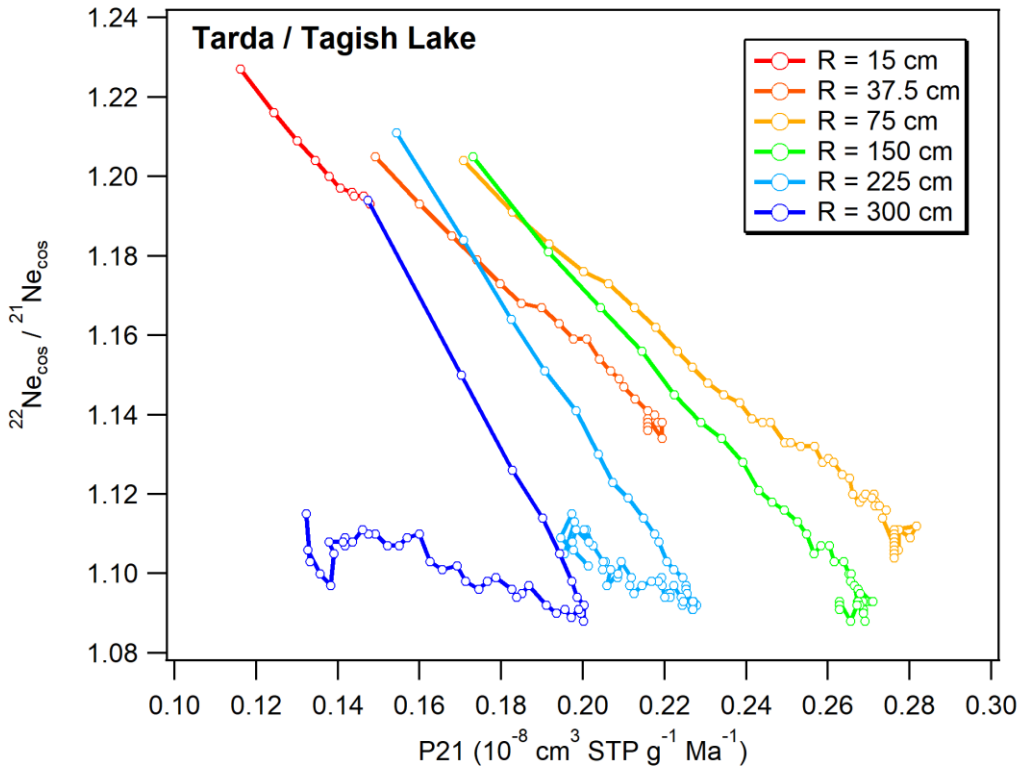


**Figure S-3** Cosmogenic $^{22}Ne/^{21}Ne$ ratio and P21 for different sizes of meteoroids (radii given in the legend) with a Tarda / Tagish Lake-like target chemistry

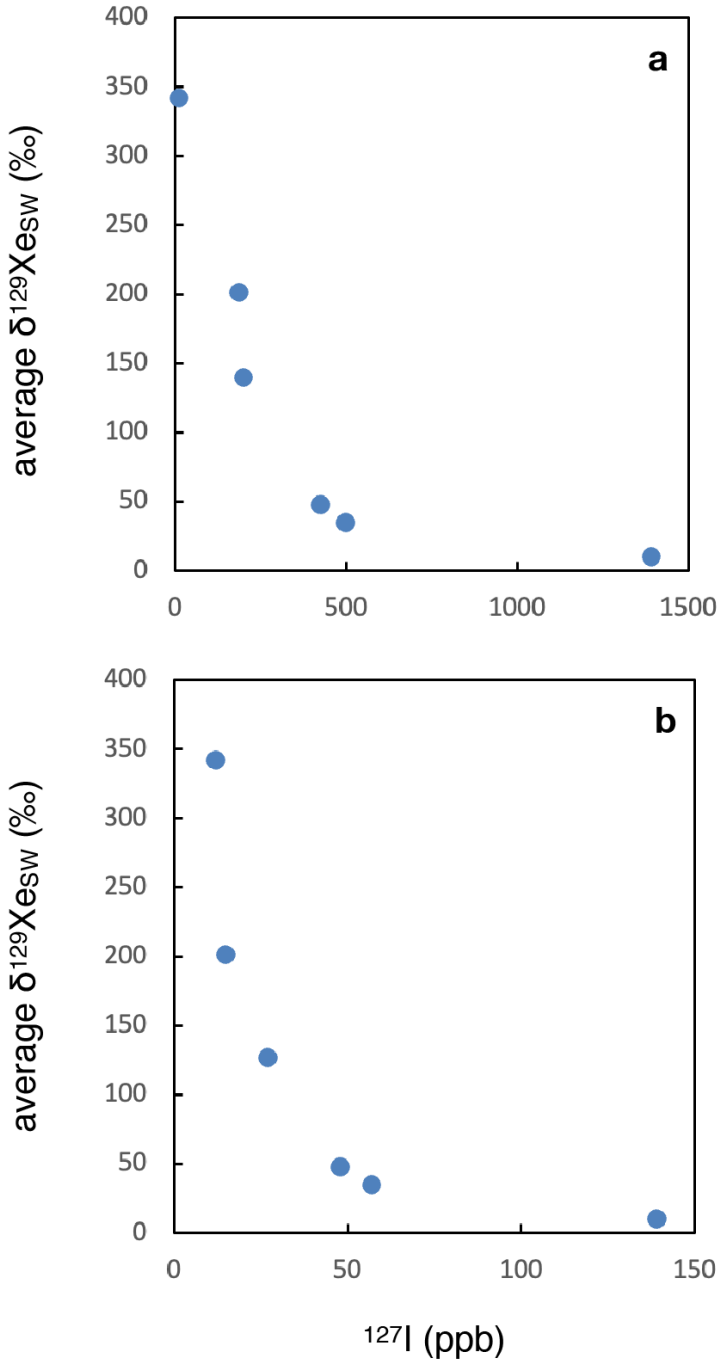


**Figure S-4** Variations of excesses of $^{129}$Xe relative to Solar Wind Xe (see also Fig. 3a) for two sets of estimates of the iodine content ($^{127}$I in ppb) of meteorites. **(a)** Iodine estimates obtained by the neutron activation method (data are from Dreibus *et al.* (1979) and Day *et al.* (2016)). **(b)** Iodine estimates obtained via the Ar-Ar method (data taken from Clay *et al.* (2017)).

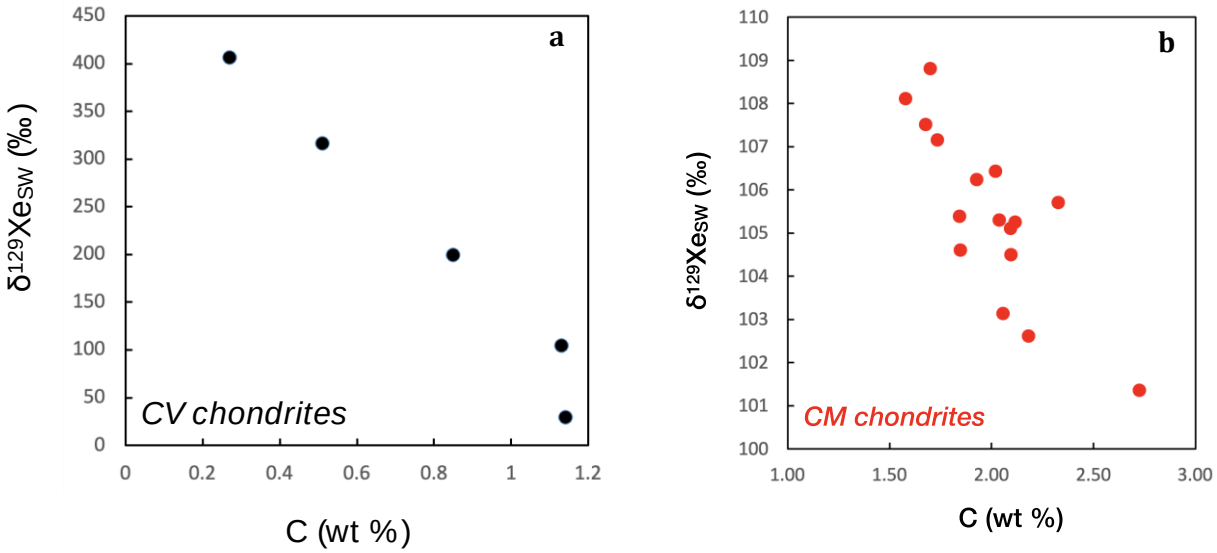


**Figure S-5** Variations of excesses of $^{129}$Xe relative to Solar Wind Xe within two meteorite groups. **(a)** CV chondrites, **(b)** CM chondrites. Data are from Alexander *et al*. (2012) and Kerridge (1985). Noble gas data are from Mazor (1970).

# Supplementary Information References


Alexander, C.M.O.'D, Bowden, R., Fogel, M.L., Howard, K.T., Herd, C.D.K., Nittler, L.R. (2012) The Provenances of Asteroids, and Their Contributions to the Volatile Inventories of the Terrestrial Planets. *Science* 337, 721–723. https://doi.org/10.1126/science.1223474

Bhandari, N., Lal, D., Rajan, R.S., Arnold, J.R., Marti, K., Moore, C.B. (1980) Atmospheric ablation in meteorites: A study based on cosmic ray tracks and neon isotopes. *Nuclear Tracks* 4, 213–262. https://doi.org/10.1016/0191-278X(80)90037-2

Brown, P.G., Hildebrand, A.R., Zolensky, M.E., Grady, M., Clayton, R.N., Mayeda, T.K., Tagliaferri, E., Spalding, R., MacRae, N.D., Hoffman, E.L., Mittlefehldt, D.W., Wacker, J.F., Bird, J.A., Campbell, M.D., Carpenter, R., Gingerich, H., Glatiotis, M., Greiner, E., Mazur, M.J., McCausland, P.JA., Plotkin, H., Mazur, T.R. (2000) The Fall, Recovery, Orbit, and Composition of the Tagish Lake Meteorite: A New Type of Carbonaceous Chondrite. *Science* 290, 320–325. https://doi.org/10.1126/science.290.5490.320

Busemann, H., Baur, H., Wieler, R. (2000) Primordial noble gases in "phase Q" in carbonaceous and ordinary chondrites studied by closed-system stepped etching. *Meteoritics and Planetary Science* 35, 949–973. https://doi.org/10.1111/j.1945-5100.2000.tb01485.x

Clay, P.L., Burgess, R., Busemann, H., Ruzié-Hamilton, L., Joachim, B., Day, J.M.D., Ballentine, C.J. (2017) Halogens in chondritic meteorites and terrestrial accretion. *Nature* 551, 614–618. https://doi.org/10.1038/nature24625

Day, J.M.D., Brandon, A.D., Walker, R.J. (2016) Highly siderophile elements in Earth, Mars, the Moon & Asteroids. *Reviews in Mineralogy and Geochemistry* 81, 161–238. https://doi.org/10.2138/rmg.2016.81.04

Dreibus, G., Spettel, B., Wänke, H. (1979) Halogens in meteorites and their primordial abundances. *Physics and Chemistry of the Earth* 11, 33–38. https://doi.org/10.1016/0079-1946(79)90005-3

Gounelle, M., Zolensky, M.E. (2014) The Orgueil meteorite: 150 years of history. *Meteoritics and Planetary Science* 49, 1769–1794. https://doi.org/10.1111/maps.12351

Kerridge, J.F. (1985) Carbon, hydrogen and nitrogen in carbonaceous chondrites: abundances and isotopic compositions in bulk samples. *Geochimica et Cosmochimica Acta* 49, 1707–1714. https://doi.org/10.1016/0016-7037(85)90141-3

Krietsch, D., Busemann, H., Riebe, M.E.I., King, A.J., Alexander, C.M.O., Maden, C. (2021) Noble gases in CM carbonaceous chondrites: Effect of parent body aqueous and thermal alteration and cosmic ray exposure ages. *Geochimica et Cosmochimica Acta* 310, 240–280. https://doi.org/10.1016/j.gca.2021.05.050

Leya, I., Masarik, J. (2009) Cosmogenic nuclides in stony meteorites revisited. *Meteoritics and Planetary Science* 44, 1061–1086. https://doi.org/10.1111/j.1945-5100.2009.tb00788.x

Marrocchi, Y., Avice, G., Barrat, J.-A. (2021) The Tarda Meteorite: A Window into the Formation of D-type Asteroids. *The Astrophysical Journal Letters* 913, 8. https://doi.org/10.3847/2041-8213/abfaa3

Mazor, E., Heymann, D., Anders, E. (1970) Noble gases in carbonaceous chondrites. *Geochimica et Cosmochimica Acta* 34, 781–824. https://doi.org/10.1016/0016-7037(70)90031-1

Ott, U. (2002) Noble Gases in Meteorites - Trapped Components. *Reviews in Mineralogy and Geochemistry* 47, 71–100. https://doi.org/10.2138/rmg.2002.47.3

Ott, U. (2014) Planetary and pre-solar noble gases in meteorites. *Chemie der Erde - Geochemistry* 74, 519–544. https://doi.org/10.1016/j.chemer.2014.01.003

Ozima, M., Podosek, F.A. (2002) Noble Gas Geochemistry. Cambridge University Press, Cambridge.